Journal of Data Acquisition and Processing
ISSN: 1004-9037
https://sjcjycl.cn/
DOI: 10.5281/zenodo.777131

# MAMMOGRAPHY IMAGES CLASSIFICATION AND DETECTION BASED ON DEEP DENSE NET CONVOLUTION GENERATIVE NEURAL NETWORK

**Mrs.T.Leena Prema Kumari**

Assistant Professor, Department of Information Technology, Fathima College, Madurai - 625018

&

Research Scholar Department of Computer Science, Madurai Kamaraj University, Madurai, TamilNadu ,India.

**Dr.K.Perumal**

Professor, Department of Computer Application, Madurai Kamaraj University, Madurai, Tamil Nadu ,India.

## ABSTRACT

Deep learning has the advantage of improved medical image processing research. Breast cancer is the most common cancer in women, and several apps have been established to improve early detection. Mammography is the most common method of screening for breast cancer, which has a high mortality rate, for women worldwide. The robustness of deep learning processes to big data strengthens the analytical abilities of Machine Learning (ML) models through feature selection on mixed image databases. Although Existing CNN-based systems have achieved higher performance than machine learning-based systems in classifying mammography images, there are several issues. These problems include ignorance of semantic features, limitations in the analysis of current image blocks, loss of blocks in low-contrast mammography images, and segmentation. These problems lead to mammography patches, computational costs, conclusions based on recent patches, and misinformation that differences in patch intensities cannot be recovered.

To overcome these issues, we proposed the method Deep Dense net Convolution Generative Neural Network ($D^2CGNN$) for using the Mammography images early detection and classification to improving the accuracy. Initially we collected the mammogram images from standard repository for malignant detection. The first pre-processing stage is based on Simple Decision Median Filter (SDMF) is used for image resizing, enhancing appearance, and reducing image noise to filter from the dataset. Then in the second step, there is a segmentation step using pre-processed image Visual Geometry Group19 (VGG) to segment the image with the aim of detecting masses in mammograms and extracting ROIs from the image. After segmentation to entering the third stage of feature selection based on Absolute Maximum Support Feature Selection (AMSFS) is used to select features based on the maximum weight

of the support section. And the VGG-19 network model is used with reduced convolutional and max pooling layers to provide a large feature dataset to classify mammograms efficiently as benign or malignant for early detection for using most support feature weights. Finally, classification is used for better accuracy. Early detection based on Deep Dense net Convolution Generative Neural Network ($D^2$CGNN) is used to evaluate the normal and abnormal images that $D^2$CGNN generates to the training data to help the classifiers avoid overfitting. Regarding validation accuracy, $D^2$CGNN is better than the image classification of previous methods.

Keywords: Deep Learning, mammograms, Breast cancer, feature weights, VGG-19, $D^2$CGNN, feature selection, classification, ROIs.

## 1. INTRODUCTION

Now a days, in medical field Breast cancer is the most common type of cancer in women, accounting for one-third of all cancers and having a mortality rate of 17%. An important factor in rising mortality is breast cancer. In order to diagnose breast cancer, mammography screening technology is crucial. Machine learning is outperforming traditional manual methods. It helps you to choose the most important features. Lumps that occur can be benign and are not considered malignant, non-cancerous, or dangerously malignant.

Benign tumors are benign, grow very slowly not spread to other main parts or invade tissue, and have well-shaped margins. However, malignant tumors can grow rapidly, invade nearby tissues, spread beyond the tumor, affect other parts of the body, lose their proper shape, and appear in unusual shapes.

Mammography is considered to be One of the best ways to detect breast cancer early isto find it. Mammography is a procedure to examine the breast using low-energy X-rays. Mammograms use x-ray images to detect the presence of disease in the breast. Mammograms clearly show the four main marks of breast cancer: lumps, micro calcifications, structural abnormalities and left-right asymmetry. However, the sensitivity of mammograms is strongly influenced by image quality, which is difficult for radiologists to interpret. Breast screening and breast screening are two types of breast examinations performed with mammography. Although mammography is designed to detect breast lesions, breast diagnosis is a follow-up examination of patients with abnormal clinical findings.

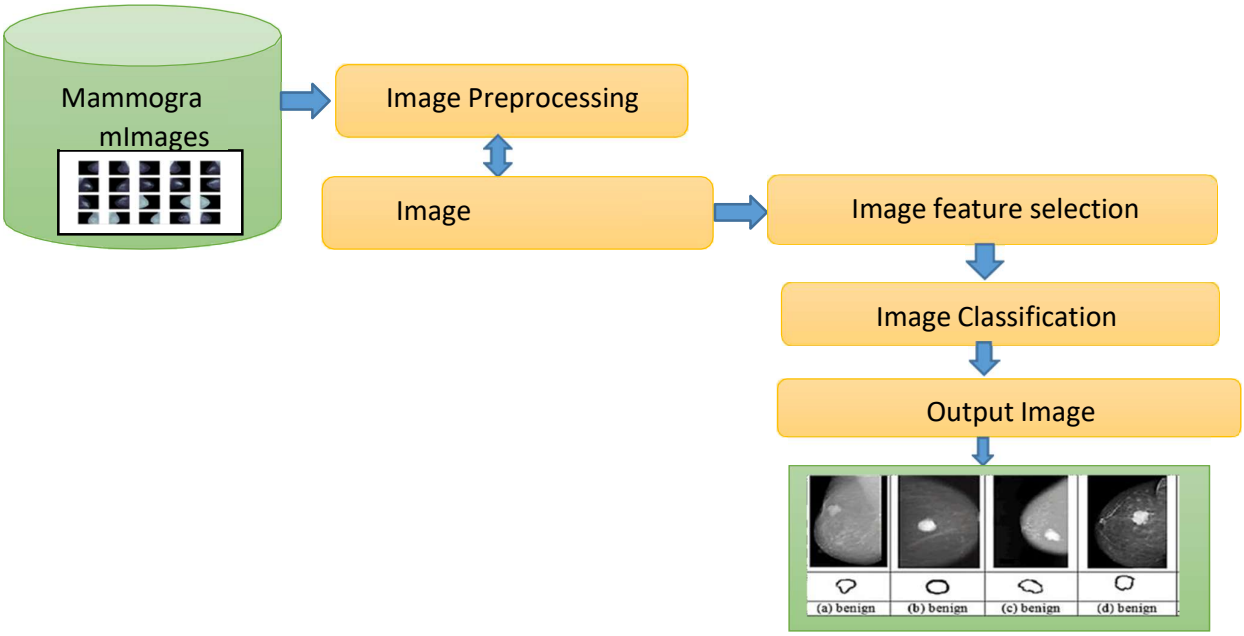


**FIGURE 1: BASIC FLOW DIAGRAM**

Figure 1 describes the basic flow of Mammography image processing based on deep learning technology classifies normal and malignant images, first collects images from Kagglelibrary and reduces noise, resizes images in pre-processing stage, before filtering, segments image region and after original image, it is selected based on features. Maximum support and the most suitable values. These image features are then used for classification to improve the accuracy and detection rate.

Deep Learning (DL) models need a larger amount of training data to achieve higher accuracy. On the other hand, medical image databases are usually small, which leads to large training errors and limits the clinical use of these models. Deep Dense net Convolution Generative Neural Network ($D^2$CGNN) method of Train a Deep Learning Model Using a Small Mammogram Dataset The images used in the dataset were used for 5 large-scale exercises, Deep Dense net Convolution Generative Neural Network ($D^2$CGNN) is build a model using transfer learning techniques. Drawing $D^2$CGNN images using a contextual attention model in the context of anomaly detection. In addition, we use a discriminative loss measure to identify areas that appear abnormal in the image-correct background. Finally, we investigate the effect of hyper parameters such as field of view and mask size on the algorithm performance.

## 2. LITERATURE SURVEY

Synthetic Digital Mammography (SDM), a two-layered picture made from a Computerized Mammography composite, is an expected choice to Full-Field Digital Mammography (FFDM) to lessen bosom radiation portion for disease screening. It is utilized restoratively as a substitute. . Past work that utilizes projection calculation and consolidates projection information with SDM blocks has involved different post-handling methods for thereprojected

information, which might bring about various picture appearance contrasted with FFDM [1]. to assess another Computer-Aided Diagnosis (CADx) convention in view of the examination of worldwide mammography picture highlights to foresee the threat capability ofa case [2].

Image synthesis is an original arrangement in accuracy medication for circumstances where basic clinical images are not accessible. Convolutional Neural Networks (CNNs) are ideal models for this undertaking because of their strong learning abilities with enormous number of layers and trainable parameters [3]. Dubious region division is one of the main pieces of the computer aided design framework for breast disease location in mammograms. Incomputer aided design frameworks, mammograms can distinguish suspicious regions due to the complex structure of the breast [4].

The patient portion for a DBT check is like that of a solitary 2D mammogram, yet securing every projection view builds the identifier readout clamor. Commotion penetrates therecreated DBT volume and can cloud unobtrusive indications of bosom malignant growth like microcalcifications (MCs) [5]. Unobtrusive contrasts in subordinate x-beam fields and x-beam lessening among ordinary and strange bosom tissue keep biomedical sensors from delivering excellent mammograms. These are normal deformities in mammography getting frameworks (sensors) that lead to unfortunate mammography picture quality [6].

Consequently analysts and researchers have carried out the improvement of PC Supported Diagnostics (CADe) and Computer Aided Diagnostics (CADx) frameworks. Conventional computer aided design frameworks depend on manual element extraction, givingradiologists unfortunate location and symptomatic apparatuses [7]. A Conditional Generative Adversarial Network (CGAN) replicates a normal-appearing mammogram, conditioned on anopposite mammogram. A Convolutional Neural Network (CNN) developed on mammograms processed by the Radon Cumulative Distribution Transform (RCDT) is used to identify MO cancers [8]. Existing multi-view based CADx frameworks regularly utilize just two perspectives: Cranio-Caudal (CC) and Medio-Lateral-Oblique (MLO). Combining data the efficiency of the mammography grouping framework, which is not possible with single-view data, is shown using data collected from two views. [9].

Lesion division requires pixel-level explanation, while infection order just requires picture level comment. The last option issue is subject to the previous, however the two undertakings are normally concentrated independently. Enlivened by their cozy relationship, we propose a half and half directed direction strategy and Residual-Aided Classification U-Net(ResCU-Net) for composite division and harmless characterization [10]. A mathematical model is accomplished by reproducing the free bosom in 3D space from pre-handled bosom forms of two perspectives [11].

Deep convolutional neural networks (DCNN) have arisen as another worldview in symptomatic mammography. Cutting edge CNN-based PC helped finding (computer aided design) frameworks for bosom malignant growth straightforwardly remove concealed highlights from input mammogram images, while ignoring the significance of morphological elements [12]. Propelled by a symmetric earlier conveyance, i.e., sores on one side of the bosom are seldom seen in comparing locales on the contrary side, we investigate responding to

counterfactual inquiries to distinguish sore regions [13].

Clinical and obsessive evaluation of this review. - In patients with okay stage I bosom malignant growth. Portion heightening examinations were intended to direct a Relative Biological Effectiveness (RBE) portion of 48.0, 52.8, or 60.0 Gy in 4 partitioned dosages more than multi week [14]. Neoadjuvant chemotherapy (NAC) has turned into a significant therapy choice for bosom malignant growth. In view of its Adverse Drug Reactions (ADRs), NAC is actually and mentally troubling. The pathologic complete reaction (pCR) file portrays patient reaction to at least six chemotherapy regimens [15].

A sum of 18 inquiries were set in the survey, which incorporated the quantity of patientstreated every year, arranging strategy, edge structure, field configuration, portion fractionationplot, hypofractionated radiotherapy use, help radiation, concurrent respective bosom radiotherapy and sped up. Halfway bosom radiotherapy. [16]. A deep convolutional brain network for bosom disease screening preliminary order was prepared and assessed on in excessof 200,000 preliminaries (a million images). Our organization accomplished an AUC of 0.895 in foreseeing the presence of bosom malignant growth when tried in a screened populace [17]. Notwithstanding customary counterfeit PC vision strategies, techniques for growth characterization utilizing deep convolutional brain organization (CNN) move learning are effectively evolved [18].

The majority of the deep learning models that are currently in use are built mostly on static breast Ultrasound (US) images. Contrast-enhanced ultrasonography is a method that radiologists frequently employ in actual diagnostic practice. Standard breast ultrasound scans lack the detail that CEUS video can, which can reveal more about the tumor's blood. distribution, thereby enabling radiologists to make more accurate diagnoses [19]. By leveraging the XGBoost framework for survival analysis, developed a gradient boosting algorithm calledBreast Cancer Disease Progression Prediction [20].

Thusly, there is a developing interest for man-made brainpower frameworks to assist specialists with settling on medical services choices, particularly with regards to perilous sicknesses. Since these frameworks are resistant to human factors, for example, interruption and stress, they recognize minor and huge issues that might be ignored, particularly in persistent outputs [21]. Just the principal preparing stage requires injury comment, and resulting stages require just picture level marking, in this manner disposing of dependence on the couple of accessible sore explanations. A completely united network way to deal with group screening mammograms accomplishes better execution contrasted with past methodologies [22].

To more readily address the distinguishing proof of irregularities in mammography images, this study utilizes a profound combination learning technique in light of pre-preparedmodels to recognize discriminative examples among typical and growth types. Planned a profound combination learning engineering for mammography image characterization [23]. Streamline the enhancement element to classify results precisely. By decreasing the bogus positive rate, the precision of the computer aided design framework has been gotten to the nextlevel. The Modified Entropy Whale Optimization Algorithm (MEWOA) is proposed a combination

based profound component extraction and characterization [24]. This approach goes about as an early recognition help for radiologists and works on the effectiveness of the framework. The Cranio Caudal (CC) and Medial Lateral Oblique (MLO) fields are broadly utilized in the ID and conclusion of bosom disease. As the quantity of online visits increments,so does the precision in identifying bosom disease. The proposed structure works in light of MLO situation and CC situation to further develop framework execution [25].

## 3. MATERIALS AND METHOD

Deep learning techniques, including mammography, thermography, ultrasound, and magnetic resonance imaging, data availability, and various breast cancer screening techniques. This section presents the dataset used in this study, where all data pre-processing methods are described, including object removal, image enhancement, and ROI extraction. An effective classifier across mammograms can result in (i) Important effort savings in marking mammograms, (ii) reduced patient turnover rates, (iii) fewer false positive cases, and reduced healthcare costs.

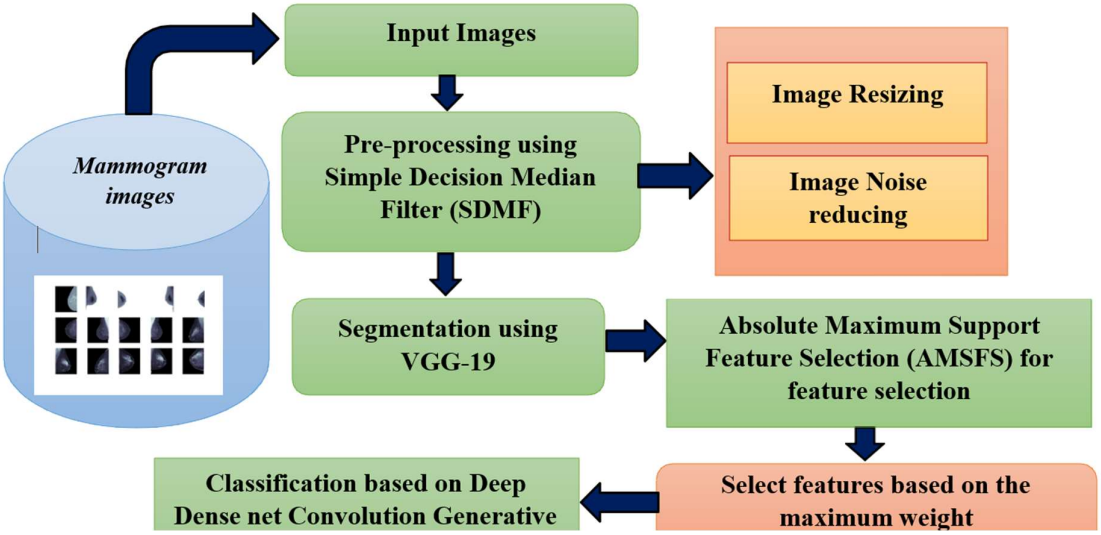


**FIGURE 2: PROPOSED BLOCK DIAGRAM FOR MAMMOGRAM IMAGE CLASSIFICATION**

Figure 2 described Mammogram Image classification using Deep learning based$D^2$CGNN. In this initial stage we collecting the dataset images from kaggle repository. So initially start the pre-processing stage for reducing noise and resizing the image to enhance theimages based on the Simple Decision Median Filter (SDMF). The second step uses the pre- processed images to segment the features using the VGG-19 method for extracting theevaluation. And another step is feature selection, selecting the feature support values from thesegmented images and estimating by their weights used for the Absolute Maximum Support Feature Selection (AMSFS). Finally, classifying the normal and abnormal images using the Deep Dense net Convolution Generative Neural Network ($D^2$CGNN) improves classification and detecting accuracy.

## COLLECTING MAMMOGRAM IMAGE

Data are images of mammography scans and labels/notations. Additional information about the database. The mammograms used in this analysis were obtained from Mammographyand Image Analysis Society (MIAS). It contains left and right chest images of 161 patients each. Three hundred twenty-two images were used for normal, non-cancerous, and infectious categories. There were 208 standard images, 63 benign images, and 51 abnormal images. The raw mammograms were 1024x1024 pixels. A radiologist reviews and interprets the mammograms.

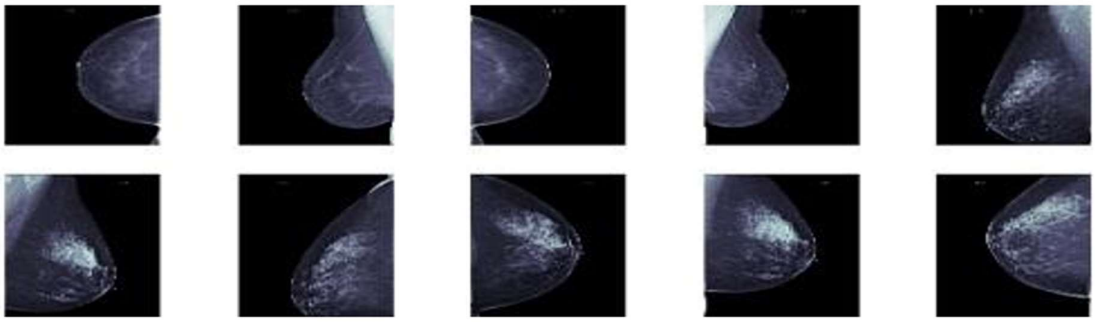

**Figure 3: Sample Images**

Figure 3 shows Sample images using features from these datasets are referenced, background tissue features: F fat, G fat gland, D dense gland, abnormal classes present: CALC calcifications, CIRC definite/limited mass, SPICS punctate mass MISC Other, Unknown Quality, ARCH Skewed Structure, ASYM Asymmetric, NORM Normal, Abnormality Severity, B Benign, M Malignant, x,y image coordinates of center of abnormality, approximate circle around abnormality in pixels radius.

## IMAGE PRE-PROCESSING BASED ON SIMPLE DECISION MEDIAN FILTER (SDMF)

Pre-processing is considered to be this is a critical step in image processing. The accuracy of this step determines the success probability of the remaining steps like segmentation, classification etc. If the unknown noise is reduced in this step, low-contrast, uneven, weak borders, and incongruent regions of the image are common features in medical images. In this **Simple Decision Median Filter (SDMF)**, together pixels are sorted according to their brightness and average rank. Eliminate irrelevant values and resizing the image compared to the neighbouring image pixel values to enhancing the image contrast level and used as part of image processing to reduce shot noise.

Inset: Mammography image Output: Pre-processed image
Step 1: Choose an image Collection of input imagesStep 2: Add noise to input image
Step 3: Using the Simple Decision Median Filter (SDMF) on Input imagesStep 4: Calculating the values PSNR (P) and MSE (M)
Step 5: Repeat 3 and 4 step for dataset images

$$PSNR(p) = 10.\log_{10}\left[\frac{M}{MSE(M)}^{2}_{1}\right] = 20.\log_{10}\left(\text{Maximum}_1 / \sqrt{MSE(m)}\right)$$

$$MSE(M) = \frac{1}{AB}\sum_{X=0}^{a-1}\sum_{y=0}^{b-1}||U(x,y) - V(x,y)||^2$$

**TABLE 1: PSNR AND MSE VALUES FOR SAMPLE IMAGES**

| Image no | Simple Decision Median Filter (SDMF) | |
|---|---|---|
| | **PSNR(P)** | **MSE(M)** |
| Img200 | 31.5714 | 64.8365 |
| Img250 | 31.120 | 60.1708 |
| Img87 | 30.8574 | 58.2701 |

Input Image Output image

**Figure 3: Sample pre-processed Images**

Figure 3 and Table 1 shows $Maximum_1$ specifies the maximum number of image pixels. If the pixel uses 8 bits per sample, then $Maximum_1$will equal 255, PSNR is used to measure the decompression quality of compressed images. Two AB monochromatic images, namely U andV, one noisy image.

## IMAGE SEGMENTATION USING VGG-19

Preprocessed images involve segmenting the visual input into segments to facilitate image segmenting based on VGG-19. A segment is a group of one or more pixels for evaluationusing Layers. Image segmentation breaks pixels into more significant components, eliminatingthe need to treat each pixel as a unit. The process of image segmentation starts by defining small areas of the image that should not be segmented.

A technique for segmenting images known as "region growing" clusters nearby pixels into regions classes where no borders are present. Due to the use of VGG-19-based selection, it is also categorized as a pixel-based image segmentation technique. The segmentation and merging approach applies to the entire image, which makes it the reverse of the segmentation method.

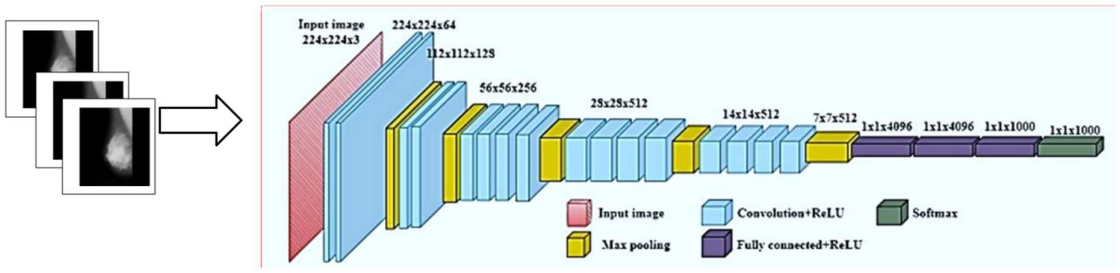


**Figure 4: Segmentation using VGG-19**

Figure 4 shows VGG-19 segmentation layers analysis the region splitting the area images. VGG-19 is a deep Learning Neural Network 19 linked layers in a network, comprising 3 fully connected layers and 16 convolutional layers. A completely convolutional layer classifies breast photos based on the attributes that a convolutional layer has extracted from the input image.

$$F_{VGG19}(1X1024) = VGG19_{(1,1)}, VGG19_{(1,2)}, \ldots VGGgg19_{(1,1024)}$$

$$\text{Max } (M), f(M) = (m_1, m_2, \ldots m_n) \in R^n, \quad m \in M$$

$R^n$ Denotes a linear independent function, n denotes the number of pixels, and M is the potential boundary region.

$$M = \{\frac{m \in R^n}{l_X \leq m_X \leq n_X}, \quad x = 1,2, \ldots, n$$

$l_X$ – Lower level image pixel values, $n_X$- upper level image pixel values,

$$M_{X,d+1} = \begin{cases} P_{X,d}, \text{ if}(p_{X,d}) \leq f(Q_{X,d}) \\ Q_{X,d}, \quad \text{otherwise} \end{cases}$$

$p_{X,d}$ To $Q_{X,d}$- using for image weights points, Utilizing a mammogram segmentation VGG-19 techniques based on the thresholding image (I) sets and pixels (P).

$$I_1 \leftarrow p_X \text{ if } 0 \leq p_X < 1$$

$$I_2 \leftarrow p_X \text{ if } th \leq p_X < p - 1$$

Maximum Region of segmentation is evaluating based on the thresholding weights, it computes the two values using mammogram images,

$$\frac{\sum_{i=0}^{X} h(x)x^2y^2}{\sum_{i=0}^{X} h(x)}$$

$\mu_1$- Image class, $x^2y^2$- pixel values, h- region of images, VGG-19 have been modified to process mammogram images,

Step for segmentation

Input: Mammographic Image (M)

Step 1: Initialize I(a, b)→loop 3x3 window $\forall(a, b)$ replace $(a, b) \rightarrow (a'v\ b')$

Step 2: Calculate the image pixel values

Step 3: The segmenting the image pixel regions

$$\frac{\text{Min distance between pixels in different group}}{\text{Max distance between pixels in same group}} X100$$

The metric used to calculate the distance processing is grayscale based; this means only numbers 0 to 254 are used. A segmentation method can separate large numbers of set regions from the original image.

## FEATURE SELECTION BASED ON ABSOLUTE MAXIMUM SUPPORT FEATURE SELECTION (AMSFS)

Features are image formats that provide some key information about an image. Feature selecting is one of the most important part of any pattern recognition application. Accuracy depends on the selection of the right features. The presence of masses in dense breast tissue and their overlapping appearance make mass classification difficult. Therefore a combination of features related to shape, contour, density and texture is preferred

To AMSFS computations, correlation features must be identified. The feature weights are calculated using the bias-increasing key technique.

Consider the two classes A and B. A and B are the feature vectors of the samples belongingto $X = (x_1, x_2, \ldots x_n)$ and$Y = (y_1, y_2, \ldots y_n)$, difference between in the $d^{th}(d = 1,2, \ldots n)$ features $d_X$ and $d_Y$ of the two samples the belongs x and y. is more, then that feature plays an important section.

$$P(d_X, d_y) = \int_{-\infty}^{+\infty} |d_X - d_y|\, f_X(d_X, d_y) p d_X * p d_y$$

Here, $f_X(d_X, d_y)$ is the random variable of the images, $d_X, d_y$-same feature valus of difference samples

$$f_X(d_X, d_y) = f_X(d_X) + f_X(d_y)$$

$$P(d_X, d_y) = \int_{-\infty}^{+\infty} |d_X - d_y|\, f_X(d_X) + f_X(d_y)\, p d_X * p d_y$$

$$P(\lambda_d) = \sum_{d=1}^{n} \lambda_d\, P(d_X, d_y)$$

Structure the model for maximizing the deviation between categories as

Follows,

$$\max P(\lambda_d) = \sum_{d=1}^{n} \lambda_d\, P(d_X, d_y)$$

Solving the model gives weight to each feature, Classification is performed using a featureset of statistical, textual and clinical data. A predictive support vector is built and trained using weighted features from the selecting features. The test models are then checked against the absolute vector matrix of test features.

Steps:

Step 1: Input sample features set f = $\{a_X, b_X\}$ x = 1 to L // where $a_X$ is features vector and

$b_X$ is the classes

Step 2: using the features constructing the vector matrix

Step 3: select the appropriate feature parameter and pixels weightsStep 4: Structure the Absolute the function

f(a) = sgn($\sum$ u = 1 to l $a_X P \times V(a_X, x) + v^*$) //$v^*$ − vector image pixels

The AMSFS algorithm based on weighted features Absolute Maximum Support Feature Selection (AMSFS) is similar to the absolute support feature vectors, except that the vector matrix absolute values is replaced by maximum feature weights.

## CLASSIFICATION BASED ON DEEP DENSE NET CONVOLUTION GENERATIVE NEURAL NETWORK($D^2$CGNN)

Classification based on Deep Dense net Convolution Generative Neural Network ($D^2$CGNN) are developed to Deep Dense net Convolution mammography images from a Digital Database of Screening Mammography (DDSM). From DTSM sets of Regions of Interest (ROIs) are

fixed out of the image: normal regions and abnormal regions (cancer/tumor). Use these ROIs to train the $D^2$CGNN and produce an artificial image.

$$\max \min_{D \quad G} (D, G) = \{\log [E_{data}(u)\}\} + P(\log \{\{1 - G|(x)|\})]\}$$

To simulate this mapping, create a neural network called generator G. If model y comesfrom $P$, $E$ data, then it is true. If the model $D$ comes from G, Another neural network detects the image pixels.

Step 1: Randomly initialize all the weights on both networks

Step 2: Feed a set of noise vectors of length 100 into the generator to get a composite image.

Step 3: Train a discriminator using synthetic images labelled "0" and real images labelled "1".

Step 4: To train the generator, feed a block of noise vectors of length 100. These synthetic images are then fed to a discriminator to obtain the predicted labels.

$$\nabla_{\theta d} \frac{1}{m} \sum_{x=1}^{n} [\log G\ (u^x) + \log (1 - I\ ((^{(x)})))]$$

$$-\nabla_{\theta d} \frac{1}{m} \sum_{x=1}^{n} [(\log (1 - I\ (G(v^{(x)})))]$$

The difference between predicted label and '1' is the loss in updating the generator. It is important to note that only the generator weights are changed during this process of constant bias weights.

## DENSE NET BLOCK WITH GENERATIVE NEURAL NETWORK

Dense blocks are used as a key part of Dense Net to improve the flow of information between layers. BN, ReLu and 3x3 transitions are included. The specific formula is as follows.$a_1 = (\{a_0, a_1, . . a_n\})$

$a_0$, $a_1$, . . $a_n$- Features mapping produces the layers, Convolutional learning features classification by extract the Features of the previous layer's output. Extracted features share the same set of weights and locks. To increase the linearity, you should pass all local weight values to the activation function.$s' = w^l . f_1(a^{l-1}) + R'$

$s'$- is the $R'$ layer neuron status, $f_1(.)$ activation function, $R'$ and $s'$ are the weightmatrix and bias from (l-1) to the $l^{th}$ function.

For number of training iterations doFor $S$ steps do
Sample of M noise samples $\{^{(1)}, \dots, . s^m\}$ noise prior

Sample of M noise samples $\{^{(1)}, \dots, . R^m\}$ data generating $D_g(M)$

Update the Generative network

$$\nabla_{\sigma a} \frac{1}{m} \sum_{x=1}^{n} [\log G\ (u^x) + \log (1 - I\ ((^{(x)})))]$$

End for

## DEEP DENSE NET CONVOLUTION GENERATIVE NEURAL NETWORK ($D^2$CGNN)

In order Classifying normal and abnormal (tumour) ROIs in DDSM, adding $D^2$CGNN-generated ROIs to training data can reduce classifier over fitting. Hence, $D^2$CGNN can be used as a preferred optimization method enhanced by $D^2$CGNN transformations cannot fully replace real images for training a CNN classifier. Lack of real images in the training set can lead to severe over fitting and requires more training.

Input: Training data (T), number of neurons N, trained **GNN** modelOutput: The label sets ($l_1$ $and\ l_2$ )
Initialize the $l_1 = \phi, l_2 = \phi$

For I =1, 2...n $S^{rt} = []$

For each $I \in D_{i0}$

End for

Find most all neurons using N, put the all values S and R

$L_i = S\emptyset\ S_i$

End For

Finally, a Softmax activation function is used because the model needs to classify threeclasses. Assume an initial learning rate of 1.0000e−04 during training.

## 4. RESULT AND DISCUSSION

The features learned from the mammography dataset are used to test the outcomes and performance of the proposed $D^2$CGNN. Performance is evaluated during the trial phase to ensure full compliance and repeatability. Computes the text case metric based on the true/false status of the implementation error rate. Performance data is a mix of positive and negative values.

**TABLE 1: SIMULATION PARAMETERS PROPOSED METHOD**

| **Using Parameters** | **Simulation Values** |
|---|---|
| Name of the dataset | Mammogram image |
| Tool | Anaconda |

| | |
|---|---|
| Language | Python |
| No. of. images | 1000 |
| Trained images | 700 |
| Testing images | 300 |

Table 1 describes A dataset of Mammogram images Processed to check validity of the proposed system. Several training and test images are evaluated for the segments to estimate the numbers for the classification

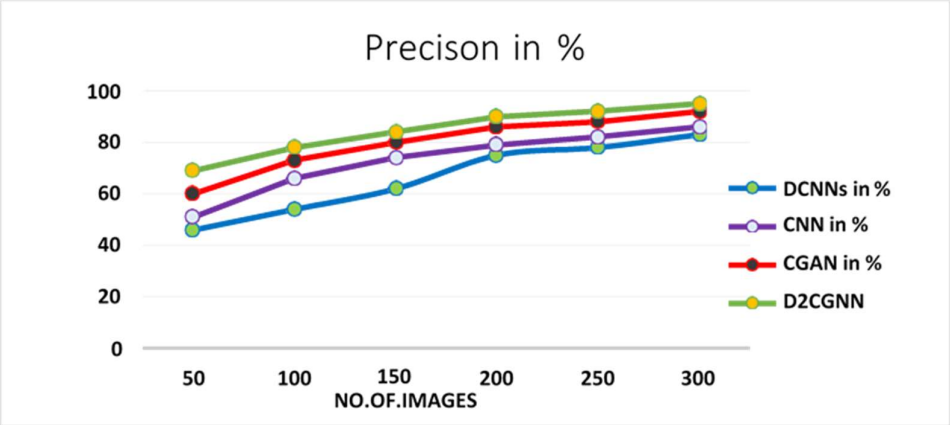


**FIGURE 3: ANALYSIS OF PRECISION RATE**

Figure 3 shows the by comparing the precision values of the actual positive rate of different methods, the proposed implementation performs better than the other methods. In theexisting methods CNN is 86%, DCNN is 92% and CGAN is 83%but the proposed method $D^2$CGNN is 95% is high precision better than previous methods

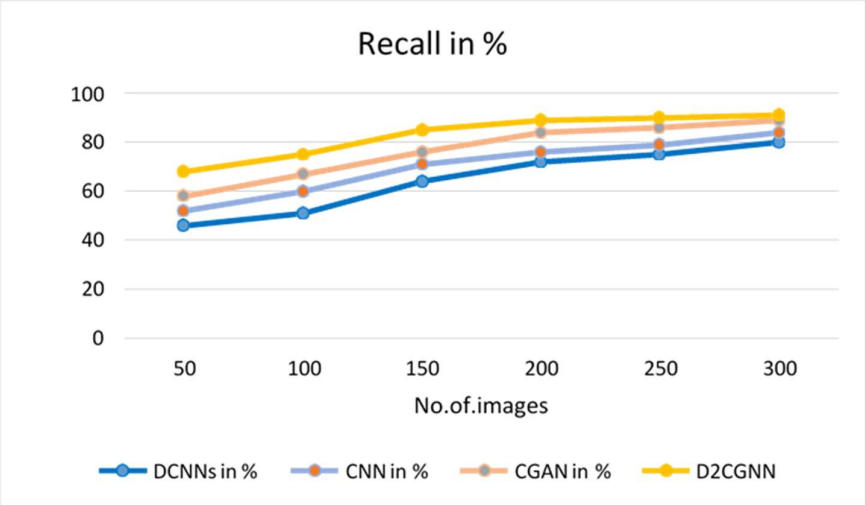


**FIGURE 4: ANALYSIS OF RECALL VALUES**

Figure 4 compares recall of true positives and false negatives for the different methods. The proposed implementation is better than other methods. In the manner that it is CNN is

84%, DCNN is 89% and CGAN is 80%but the proposed method is D2CGNN 91% is high recall better than previous methods.

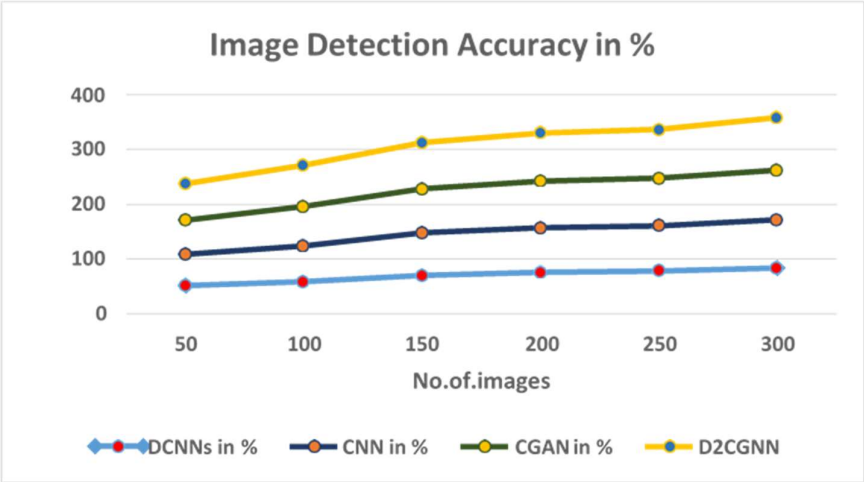


**FIGURE 5: ANALYSIS OF IMAGE DETECTION ACCURACY**

Figure 5 describes to comparing the image detection accuracy values of the various methods, the proposed implementation shows higher performance compared to other algorithms. In existing methods, DCNN is 88%, CNN is 90%, and CGAN is 84%, whereas ourproposed method $D^2$CGNN, the recall is 96% higher, which is better than previous methods.

## 5. Conclusion

In the field of medical imaging, extracting features and classifying images based on the optimized features is the main area where deep learning programs are used. Apply machine learning classifiers to yield more useful outcomes. Deep Dense Net Convolution Generative Neural Network (D2CGNN) uses unbalanced datasets in the proposed work. Using an average pooling layer, deep characteristics are extracted. a quick way to determine whether a ROI is benign or cancerous. The pre-trained D2CGNN model serves as the foundation of the suggested approach. Transfer the pre-trained functions to new classes rather than eliminating completely connected layers and introducing new problem-specific layers, as indicated in the literature. The suggested strategy identifies the most active neurons in the last fully connected layer and makes use of these operations to categorize a new, substantial number of ROIs. There is only one convolutional layer serving as a feature extractor in the suggested custom model. The accuracy of the unique model is 96%. The custom models train more quickly than any other model and with fewer training parameters. Future plans call for the model to be tested against new ultrasound images and other datasets.

## Reference

1. G. Jiang et al., "Synthesis of Mammogram From Digital Breast Tomosynthesis Using Deep Convolutional Neural Network With Gradient Guided cGANs," in IEEE Transactions on Medical Imaging, vol. 40, no. 8, pp. 2080-2091, Aug. 2021, doi: 10.1109/TMI.2021.3071544.

2. M. Heidari, S. Mirniaharikandehei, W. Liu, A. B. Hollingsworth, H. Liu and B. Zheng, "Development and Assessment of a New Global Mammographic Image Feature

Analysis Scheme to Predict Likelihood of Malignant Cases," in IEEE Transactions on Medical Imaging, vol. 39, no. 4, pp. 1235-1244, April 2020, doi: 10.1109/TMI.2019.2946490.

3. F. Gao, T. Wu, X. Chu, H. Yoon, Y. Xu and B. Patel, "Deep Residual Inception Encoder–Decoder Network for Medical Imaging Synthesis," in IEEE Journal of Biomedical and Health Informatics, vol. 24, no. 1, pp. 39-49, Jan. 2020, doi: 10.1109/JBHI.2019.2912659.

4. M. Gao, J. A. Fessler and H. -P. Chan, "Deep Convolutional Neural Network With Adversarial Training for Denoising Digital Breast Tomosynthesis Images," in IEEE Transactions on Medical Imaging, vol. 40, no. 7, pp. 1805-1816, July 2021, doi: 10.1109/TMI.2021.3066896.

5. H. El Malali, A. Assir, V. Bhateja, A. Mouhsen and M. Harmouchi, "A Contrast Enhancement Model for X-Ray Mammograms Using Modified Local s-Curve Transformation Based on Multi-Objective Optimization," in IEEE Sensors Journal, vol. 21, no. 10, pp. 11543-11554, 15 May15, 2021, doi: 10.1109/JSEN.2020.3028273.

6. J. Lee and R. M. Nishikawa, "Identifying Women With Mammographically- Occult Breast Cancer Leveraging GAN-Simulated Mammograms," in IEEE Transactions on Medical Imaging, vol. 41, no. 1, pp. 225-236, Jan. 2022, doi: 10.1109/TMI.2021.3108949.

7. H. Nasir Khan, A. R. Shahid, B. Raza, A. H. Dar and H. Alquhayz, "Multi-View Feature Fusion Based Four Views Model for Mammogram Classification Using Convolutional Neural Network," in IEEE Access, vol. 7, pp. 165724-165733, 2019, doi: 10.1109/ACCESS.2019.2953318.

8. T. Shen, C. Gou, J. Wang and F. -Y. Wang, "Simultaneous Segmentation and Classification of Mass Region From Mammograms Using a Mixed-Supervision Guided Deep Model," in IEEE Signal Processing Letters, vol. 27, pp. 196-200, 2020, doi: 10.1109/LSP.2019.2963151.

9. X. Duan et al., "Matching Corresponding Regions of Interest on Cranio-Caudal and Medio-Lateral Oblique View Mammograms," in IEEE Access, vol. 7, pp. 31586- 31597, 2019, doi: 10.1109/ACCESS.2019.2902854.

10. H. Li, D. Chen, W. H. Nailon, M. E. Davies and D. I. Laurenson, "Dual Convolutional Neural Networks for Breast Mass Segmentation and Diagnosis in Mammography," in IEEE Transactions on Medical Imaging, vol. 41, no. 1, pp. 3-13, Jan. 2022, doi: 10.1109/TMI.2021.3102622.

11. C. Wang et al., "Bilateral Asymmetry Guided Counterfactual Generating Network for Mammogram Classification," in IEEE Transactions on Image Processing, vol. 30, pp. 7980-7994, 2021, doi: 10.1109/TIP.2021.3112053.

12. Zahoor S, Shoaib U, Lali IU. Breast Cancer Mammograms Classification Using Deep Neural Network and Entropy-Controlled Whale Optimization Algorithm. Diagnostics (Basel). 2022 Feb 21;12(2):557. doi: 10.3390/diagnostics12020557. PMID: 35204646; PMCID: PMC8871265.

13. Wessam M. Salama, Moustafa H. Aly, Deep learning in mammography images segmentation and classification: Automated CNN approach, Alexandria Engineering

Journal, Volume 60, Issue 5, 2021, Pages 4701-4709, ISSN 1110-0168, https://doi.org/10.1016/j.aej.2021.03.048.

14. G. Toz and P. Erdoğmuş, "A Novel Hybrid Image Segmentation Method for Detection of Suspicious Regions in Mammograms Based on Adaptive Multi-Thresholding (HCOW)," in IEEE Access, vol. 9, pp. 85377-85391, 2021, doi: 10.1109/ACCESS.2021.3089077.

15. F. Azour and A. Boukerche, "Design Guidelines for Mammogram-Based Computer-Aided Systems Using Deep Learning Techniques," in IEEE Access, vol. 10, pp. 21701-21726, 2022, doi: 10.1109/ACCESS.2022.3151830.

16. T. Kretz, K. -R. Müller, T. Schaeffter and C. Elster, "Mammography Image Quality Assurance Using Deep Learning," in IEEE Transactions on Biomedical Engineering, vol. 67, no. 12, pp. 3317-3326, Dec. 2020, doi: 10.1109/TBME.2020.2983539.

17. Z. Ning, S. Zhong, Q. Feng, W. Chen and Y. Zhang, "SMU-Net: Saliency-Guided Morphology-Aware U-Net for Breast Lesion Segmentation in Ultrasound Image," in IEEE Transactions on Medical Imaging, vol. 41, no. 2, pp. 476-490, Feb. 2022, doi: 10.1109/TMI.2021.3116087.

18. G. Mettivier et al., "In-Line Phase Contrast Mammography, Phase Contrast Digital Breast Tomosynthesis, and Phase Contrast Breast Computed Tomography With a Dedicated CT Scanner and a Microfocus X-Ray Tube: Experimental Phantom Study," in IEEE Transactions on Radiation and Plasma Medical Sciences, vol. 5, no. 6, pp. 793- 806, Nov. 2021, doi: 10.1109/TRPMS.2020.3003380.

19. W. C. Walton, S. -J. Kim and L. A. Mullen, "Automated Registration for Dual-View X-Ray Mammography Using Convolutional Neural Networks," in IEEE Transactions on Biomedical Engineering, vol. 69, no. 11, pp. 3538-3550, Nov. 2022, doi: 10.1109/TBME.2022.3173182.

20. M. Tardy and D. Mateus, "Looking for Abnormalities in Mammograms With Self- and Weakly Supervised Reconstruction," in IEEE Transactions on Medical Imaging, vol. 40, no. 10, pp. 2711-2722, Oct. 2021, doi: 10.1109/TMI.2021.3050040.

21. A. Aminzadeh et al., "Imaging Breast Microcalcifications Using Dark-Field Signal in Propagation-Based Phase-Contrast Tomography," in IEEE Transactions on Medical Imaging, vol. 41, no. 11, pp. 2980-2990, Nov. 2022, doi: 10.1109/TMI.2022.3175924.

22. G. Matrone, M. A. L. Bell and A. Ramalli, "Spatial Coherence Beamforming With Multi-Line Transmission to Enhance the Contrast of Coherent Structures in Ultrasound Images Degraded by Acoustic Clutter," in IEEE Transactions on Ultrasonics, Ferroelectrics, and Frequency Control, vol. 68, no. 12, pp. 3570-3582, Dec. 2021, doi: 10.1109/TUFFC.2021.3099730.

23. S. Zhao et al., "Ultrashort-Pulse-Microwave Excited Whole-Breast Thermoacoustic Imaging With Uniform Field of Large Size Aperture Antenna for Tumor Screening," in IEEE Transactions on Biomedical Engineering, vol. 69, no. 2, pp. 725-733, Feb. 2022, doi: 10.1109/TBME.2021.3104137.

24. G. Umezu, Y. Yamauchi and S. Kidera, "Contrast Source Inversion Enhanced Confocal Imaging for Highly Heterogeneous Breast Media in Microwave Mammography," in

IEEE Journal of Electromagnetics, RF and Microwaves in Medicine and Biology, vol. 6, no. 4, pp. 494-500, Dec. 2022, doi: 10.1109/JERM.2022.3196504.

25. B. Wang, X. Hu, J. Zhang, C. Xu and Z. Gao, "Intelligent Internet of Things in Mammography Screening Using Multicenter Transformation Between Unified Capsules," in IEEE Internet of Things Journal, vol. 10, no. 2, pp. 1536-1545, 15 Jan.15, 2023, doi: 10.1109/JIOT.2022.3209895.